Measurement of pediatric regional cerebral blood flow from 6 months to 15 years of age in a clinical population

Aline Carsin-Vu, Isabelle Corouge, Olivier Commowick, Guillaume Bouzillé, Christian Barillot, Jean-Christophe Ferré, Maia Proisy

TITLE:

Measurement of pediatric regional cerebral blood flow from 6 months to 15 years of age in a clinical population

Authors:

Aline Carsin-Vu [a-e], Isabelle Corouge [a-d], Olivier Commowick [a-d], Guillaume Bouzillé [f,g] Christian Barillot [a-d], Jean-Christophe Ferré [a-d,h], Maia Proisy [a-d,h]

Authors affiliations and addresses:

[a] *Univ Rennes1, Faculté de médecine, F-35043 Rennes, France*

[b] *INSERM, U 1228, ERL VISAGES, F-35042 Rennes, France*

[c] *CNRS, IRISA, UMR 6074, F-35042 Rennes, France*

[d] *INRIA, VISAGES project-team, F-35042 Rennes, France*

[e] *CHU Reims, Département de radiologie, F-51092 Reims, France*

[f] *INSERM, U 1414, CIC, F-35033 Rennes, France*

[g] *CHU Rennes, Centre de Données Cliniques, F-35033 Rennes, France*

[h] *CHU Rennes, Département de radiologie, F-35033 Rennes, France*

Grant support:

Aline Carsin-Vu received a research grant from the French Society of Radiology. The funding source was not involved in the study design; in the collection, analysis or interpretation of data; in the writing of the report.

Conflict of interest:

The authors have no conflicts of interest.

ABSTRACT:

Objectives: To investigate changes in cerebral blood flow (CBF) in gray matter (GM) between 6 months and 15 years of age and to provide CBF values for the brain, GM, white matter (WM), hemispheres and lobes.

Methods: Between 2013 and 2016, we retrospectively included all clinical MRI examinations with arterial spin labeling (ASL). We excluded subjects with a condition potentially affecting brain perfusion. For each subject, mean values of CBF in the brain, GM, WM, hemispheres and lobes were calculated. GM CBF was fitted using linear, quadratic and cubic polynomial regression against age. Regression models were compared with Akaike's information criterion (AIC), and Likelihood Ratio tests.

Results: 84 children were included (44 females/ 40 males). Mean CBF values were 64.2 ± 13.8 mL/100g/min in GM, and 29.3 ± 10.0 mL/100g/min in WM. The best-fit model of brain perfusion was the cubic polynomial function (AIC = 672.7, versus respectively AIC = 673.9 and AIC = 674.1 with the linear negative function and the quadratic polynomial function). A statistically significant difference between the tested models demonstrating the superiority of the quadratic ($p = 0.18$) or cubic polynomial model ($p = 0.06$), over the negative linear regression model was not found. No effect of general anesthesia ($p = 0.34$) or of gender ($p = 0.16$) was found.

Conclusion: we provided values for ASL CBF in the brain, GM, WM, hemispheres, and lobes over a wide pediatric age range, approximately showing inverted U-shaped changes in GM perfusion over the course of childhood.

KEYWORDS:

Arterial spin labeling (ASL); pediatric brain imaging; cerebral blood flow (CBF).

ABBREVIATIONS:

(p)ASL, (pulsed) arterial spin labeling; MRI, magnetic resonance imaging; CBF, cerebral blood flow; GM, gray matter; WM, white matter; CSF, cerebrospinal fluid; ROIs, regions of interest; AAL, automated anatomical labeling; AIC, Akaike's information criterion; LRT, likelihood ratio tests.

HIGHLIGHTS:

- ASL technique is an innovative non-radiating and non-invasive method to quantify CBF.
- We provide ASL CBF values for GM and WM between 6 months and 15 years of age.
- GM CBF seems to increase up to 3-4 years of age and decline thereafter.
- There was no influence of gender and general anesthesia on CBF during childhood.

TEXT

1. Introduction

Arterial Spin Labeling (ASL), developed in the early 1990s, is an innovative magnetic resonance imaging (MRI) sequence that uses magnetically labeled protons of blood water as an endogenous contrast agent [1]. It enables imaging of brain perfusion and quantification of cerebral blood flow (CBF) without intravenous injection or irradiation, unlike nuclear medicine or MRI-based perfusion techniques involving injection of a paramagnetic contrast agent. Consequently, ASL is particularly well suited for investigating pediatric brain perfusion.

From birth to adulthood, the brain undergoes many overall and regional developmental changes. The ability to study these transformations would allow a better understanding of brain development. A possible way to do this could be the quantification of CBF using ASL due to its non-invasive nature and the close relationship between cerebral metabolism and perfusion [2]. ASL is also increasingly used in pathological contexts [3], particularly for newborn hypoxic-ischemic encephalopathy [4], cerebrovascular diseases [5], epilepsy, brain tumor grading and tumor identification [3,6].

ASL is not yet widely used as a routine perfusion method. One of the reasons for this is the incomplete knowledge of normal pediatric ASL CBF values and the potential changes in brain perfusion over the course of childhood. This knowledge is a prerequisite for the pertinent detection of CBF abnormalities. Several teams have studied CBF in pediatric populations using ASL but these studies were often limited to specific age groups, around birth [7,8] or after 4 years of age [9–12]. To our knowledge, there is only one study that reports CBF values using ASL in four

subjects aged between 6 months and 4 years [13]. In this age group, sedation or general anesthesia is virtually mandatory to obtain the child's compliance, and this could have distorted the results of the investigation. Consequently, there is a real need to investigate normal CBF values in a wide range of ages in order to develop clinical use of ASL in the pediatric population and to better understand brain development.

The aim of this study was to investigate changes in brain perfusion in gray matter from 6 months to 15 years of age, using ASL sequences, and to provide reference values for the brain, gray matter (GM), white matter (WM), hemispheres, and lobes in this age range. A secondary objective was to study the effect of general anesthesia and gender on CBF values.

2. Material and methods

2.1. Study population

We retrospectively reviewed all consecutive routine brain MRIs performed in our pediatric radiology department between January 2013 and June 2016 for which ASL images had been acquired. The main inclusion criteria were age between 6 months and 15 years and normal morphological MRI images. The main exclusion criteria were all factors that could have affected CBF such as a history of stroke, brain tumor, metabolic diseases, seizure or headache in the previous 2 days, prematurity, brain malformations or neurosurgery. MRI indications were resumed in Table 1. We excluded scans with artifacts or significant patient movement. The study was approved by the local Institutional Review Board. According to national legislation, written consent is not necessary for such retrospective studies, however all the parents were informed about the study and could choose not to include their child.

2.2. MRI protocol

All scans were performed on a 1.5 T Magnetom Aera (Siemens Healthcare, Erlangen, Germany) with a 12-channel head coil. The complete imaging protocol varied according to clinical features but 3D T1-weighted and pulsed ASL (pASL) images were acquired in all cases. The parameters of both image types were standardized.

The parameters of 3D sagittal MPRAGE T1-weighted morphological images were as follows: TR = 2090 ms, TE = 4.92 ms, TI = 1100 ms, 256 × 256 matrix, 0.5 × 0.5 × 1 mm^3 voxel size, FOV = 26 cm^2, 160 slices, TA = 200 s.

The parameters of pASL axial images with the PICORE Q2TIPS labeling scheme [14] were as follows: TR = 3200 ms, TE = 12 ms, TI_1/TI_2 = 700/1800 ms, 64 × 64 matrix, 4 × 4 × 8 mm^3 voxel size, FOV = 256 mm^2, TA = 336 s, 9 slices, 8 mm

slice thickness, 2.0 mm slice gap, 61 repetitions. One M_0 reference image (magnetization of brain tissue at the equilibrium used to normalize the difference perfusion map) and 30 control/label image pairs were acquired.

Depending on the age and behavior of children, sedation or general anesthesia was administered before performing the scan as required. A pediatrician performed sedation with permanent monitoring of oxygen saturation. The general anesthesia protocol was standardized using sevoflurane. A controlled ventilation system and an end-tidal carbon dioxide monitor were used to maintain normocapnia.

2.3. Data processing

Processing of both 3D-T1 and ASL images was performed using custom-built ASL processing tools based on SPM8 (Wellcome Trust Centre for Neuroimaging, Institute of Neurology, University College, London, UK) and MATLAB® 2014b (The MathWorks Inc., Natick, Massachusetts, USA).

2.3.1. Anatomical data processing

Brain data were extracted with the FSL Brain Extraction Tool (Analysis Group, FMRIB, Oxford, UK) [15]. A bias intensity correction of each T1-weighted sequence was performed using SPM. Then the sequence was segmented into GM, WM and cerebrospinal fluid (CSF) probability maps using NIHPD pediatric brain atlases [16]. Spatial normalization parameters, estimated by the same unified segmentation model SPM routine, were applied to register the 3D T1 volumes to the atlas space.

2.3.2. ASL data processing

The first step was a 6-parameter (rigid body) registration of the ASL volumes acquired from the same subject using a least-squares approach to reduce subject motion between repetitions [17]. Then the M0 image was separated from other ASL volumes; label and control volumes were pair-wise subtracted. The perfusion signal was usually obtained by averaging across the repetitions. However, a conventional mean is sensitive to outliers. To create a perfusion-weighted map, we replaced the conventional mean by a Huber-M-estimator, that minimizes the weight of a repetition far removed from the mean [18]. Then the perfusion-weighted map was co-registered to the 3D T1 gray matter map using a rigid transform and by maximizing Normalized Mutual Information. The averaged perfusion-weighted map was converted into a quantitative ASL CBF map by applying the following single compartment model [13,19]:

$$\mathrm{CBF} = \frac{6000 \times \lambda \times \Delta M \times e^{\frac{(TI_2 + idx_{sl} \times TI_{sl})}{T_{1b}}}}{2 \times \alpha \times TI_1 \times M_{0b}} \left[\mathrm{mL}/100\mathrm{g}/\mathrm{min}\right]$$

The factor of 6000 converts the unit from mL/g/s to mL/100g/min. λ is the brain/blood partition coefficient in mL/g (0.9 mL/g) [20]. ΔM is the average difference in signal intensity between control and label acquisitions. TI_2, inversion time, is the time from the initial pulse to image acquisition (1800 ms) [20]. TI_2 is adjusted for each slice to take into consideration the time interval TI_{sl} (47 ms) between slice acquisitions in our 2D multislice ASL sequences. idx_{sl} is the slice index (0 for the first slice). Blood T1, T_{1b}, is the longitudinal relaxation time of blood in seconds (1350 ms). Alpha is labeling efficiency (98%) [20]. TI_1 is the duration between the inversion and

saturation pulse (700 ms). M_{0b} is the longitudinal magnetization of blood at equilibrium and is estimated from the M0 map, the first volume of the ASL series. Finally, the normalization step warped each individual quantitative ASL CBF map using the spatial normalization parameters estimated from the anatomical data normalization and a smoothing process applied a smoothing filter to the images.

2.3.3. Regions of interest (ROIs) analysis in brain tissues

By applying as masks the GM and WM probability map obtained during anatomical data processing, it was possible to create GM and WM ASL CBF maps for each subject in GM and WM. To avoid cross-contamination between brain tissue, we thresholded GM and WM probability maps at 80% and 99 % respectively prior to masking [21]. Overall CBF values were obtained by averaging GM and WM CBF maps subsequent to masking. The quality of the segmentation was visually checked.

2.3.4. Regions of interest analysis (ROIs) in lobes and hemispheres

Lobe (frontal, temporal, parietal, occipital, limbic and insular) and hemisphere masks were defined using the Automated Anatomical Labeling (AAL) atlas [22]. Lobe definitions are summarized in the appendix. Hemispheres were defined by all the right and left regions available in AAL. CBF values were averaged in each lobe and hemisphere ROIs using masks created with AAL and the GM CBF map. Given that the ASL sequence may not completely cover supratentorial regions, the lobe GM CBF maps had to contain lobe volumes greater than 10 cm^3 in the insular lobe, 20 cm^3 in the limbic lobe, 35 cm^3 in the occipital lobe, 60 cm^3 in the parietal lobe, 40 cm^3 in the temporal lobe and 100 cm^3 in the frontal lobe to be taken into consideration. Threshold values were chosen by rounding half of the average of GM CBF map

lobes volumes in our population. The quality of the segmentations was visually checked.

2.4. Statistical analysis

Quantitative (continuous) data were expressed as mean ± standard error of the means. Qualitative data were expressed as numbers and percentages.

We performed an analysis to study the relationships between grey matter CBF values and the potential associated factors. CBF values in GM were plotted against age and fitted using linear, quadratic and cubic polynomial regression. We evaluated the goodness of fit of the models with the use of Akaike's information criterion (AIC), defined as: AIC = - 2 ln *L* + 2 p, where L is the penalized maximum likelihood and p is the number of parameters. The AIC has the advantage of minimizing potential overfitting issues caused by incorporating too many parameters in the models (the smaller the value of this statistic, the better the model). We used Pearson correlation tests for each model. We also performed Likelihood Ratio tests (LRT) between models. We investigated the influence of hemisphere side on CBF using a paired student's t-test. We used a student's t-test to study the association with gender and general anesthesia after ensuring that the variables were normally distributed. For multiple comparisons between GM CBF in lobes, data were analyzed with a two-factor repeated-measures analysis of variance (ANOVA) between lobes. Post hoc comparisons were performed by Tukey's honestly significant difference test to specify differences among mean GM CBF values in lobes. We considered a two-sided *p* value of less than 0.05 as statistically significant. We performed the statistical analysis using R© 3.2.4 statistical computing software (R Core Team (2017). R: A

language and environment for statistical computing. R Foundation for Statistical Computing, Vienna, Austria. URL https://www.R-project.org/).

3. Results

3.1. Population

We reviewed approximatively 600 MRI scans, and 90 patients met our inclusion criteria. Six parents chose not to include their child. Eighty-four children were finally included, distributed equally: 44 females (52%), and 40 males (48%). Their mean age was 7.2 years (range: 6 months - 15 years and 10 months). The age distribution of the children is shown in Table 2. Forty-one children received no sedation (49%), 16 (19%) needed general anesthesia and 27 (32%) received a sedative.

3.2. Age-related changes in brain perfusion

CBF was 64.2 ± 1.5 mL/100g/min in GM, and 29.3 ± 1.1 mL/100g/min in WM. The CBF values in the brain, gray matter, white matter and hemispheres per age group class are summarized in Table 2.

CBF values in gray matter are plotted against age in Figure 1. CBF in GM seemed to increase from 6 months to 3-4 years of age and declined thereafter. The equations of the polynomial models fitted (linear, quadratic and cubic) to the GM CBF values with respect to age (years) were as follows:

1. linear model: GM CBF = 71.50 – 1.01 × age
2. quadratic model: GM CBF = 67.86 + 0.49 × age - 0.09 × age^2
3. cubic model: GM CBF = 60.74 + 5.82 × age - 0.92 × age^2 + 0.03 × age^3

The best-fit-model of brain perfusion was the cubic polynomial function (AIC = 672.7, versus AIC = 673.9 with the negative linear function and AIC = 674.1 with the quadratic polynomial function). However, we did not find a statistically significant difference between the three tested polynomial regression models that would have

demonstrated the superiority of the quadratic or cubic polynomial model over the negative linear regression model (Table 3).

No significant difference was found between mean CBF of left and right hemispheres (GM CBF: right hemisphere 65.3 ± 1.6 mL/100g/min versus left hemisphere 64.8 ± 1.5 mL/100g/min; $p = 0.09$); therefore, right and left hemispheres were combined for analysis per lobe. CBF values in lobes per age group are summarized in Table 4. CBF was often highest in the occipital lobe and lowest in the limbic and insular lobe in most age group. Two-factor repeated-measures ANOVA showed a significant effect of lobes in GM CBF between 6 months and 15 years of age ($p < 0.0001$). After ANOVA, the Tukey's honestly significant difference test only indicated significant differences of GM CBF between occipital lobe and parietal, frontal, insular or limbic lobe (respectively $p = 0.01$, $p = 0.002$, $p < 0.0001$, $p < 0.0001$) and between temporal lobe and limbic or insular lobe (respectively $p = 0.002$, $p = 0.0002$) (Figure 3).

3.3. Effect of general anesthesia and gender on cerebral blood flow

In GM, CBF was not significantly different between females and males (62.1 ± 2 mL/100g/min versus 66.4 ± 2.2 mL/100g/min; $p = 0.16$). No significant effect of general anesthesia was found. Mean GM CBF was 64.9 ± 1.7 mL/100g/min without general anesthesia and 61.2 ± 3.4 mL/100g/min with general anesthesia, $p = 0.34$.

4. Discussion

Knowledge of normal pediatric CBF values is vital for improving our understanding of normal human brain development and the accuracy of diagnosis of pediatric brain pathologies. To the best of our knowledge, this study investigates normal pediatric CBF changes using ASL MRI perfusion over the widest age range reported in the literature to date, covering the period from infancy to adolescence. The obtained CBF values should be helpful in pathological context [3] such as migraine, Sickle cell disease…

The GM CBF measured by the ASL images tended to increase during the first years of life with a peak at 3-4 years, and to progressively decline afterwards, following an approximatively inverse U-shaped curve. During late adolescence, CBF seemed to display a small rebound. The superiority of the cubic polynomial function over the linear or quadratic function for fitting GM CBF with age was not significant, probably because of a lack of power due to our relatively small sample size. However, the third-order polynomial model had the smallest AIC, which means this model is likely to have the best performance for predicting future observations. Previous studies described similar inverse U-shaped changes in brain perfusion over the course of childhood generally, produced with several imaging techniques: SPECT using ^{133}Xe [23] in brain, perfusion CT [24] in GM and ASL MRI [10] in most lobes. In the latter study [10], the CBF peak occurred later but the age range of its population was higher (5-18 years). A parallel age-related evolution of local cerebral metabolic rate of glucose by PET was shown by Chugani et al [25]. The teams studying ASL MRI with smaller age ranges found a similar CBF increase after birth [8] and CBF reduction after 7 years of life [9,11,12,26]. A small rebound of CBF values during late

adolescence was also noticed by Taki et al [10] in some brain regions. Considering the close relationship between CBF and glucose consumption, the CBF rising phase could correspond to the overproduction of neurons and synapses during the first years of life and the second phase to the decrease in the number of synapses per neuron [10,23,25].

On the basis of literature providing absolute values of CBF determined with the ASL images in children above 4 years of age, the mean GM CBF varies from 62 to 96.5 mL/100g/min, and mean WM CBF varies from 22 to 41.58 mL/100g/min [9,27,11,12]. Our GM CBF values were in the lower range, and WM CBF values were of the same order. The highest regional CBF values were found in occipital lobes, in common with Duncan et al [8] and in the contrast to other studies [10,27]. Nevertheless, it is difficult to compare our regional CBF values to those in the literature because of differences in age groups and different methodological issues for brain region definition and ROI measurements (manual or automatic).

We did not find a significant effect of gender on brain perfusion during childhood, in common with Duncan et al with ASL between 3 and 5 months of age, and Wintermark et al with perfusion CT during childhood [8,24]. Nonetheless, Satterthwaite et al [26] found a gender difference for CBF changes over time from mid puberty in many brain regions, particularly in hubs of the default mode network and executive system: female CBF described a plateau before an increase from around 14-15 years, although male CBF continued to decrease until adulthood. The upper limit of our age group was in mid puberty and this could explain the absence of a significant gender influence.

Very few studies have investigated the influence of anesthesia on ASL CBF in a pediatric population. General anesthesia is known to usually induce depression of

CBF and of metabolism [28]. Unlike a previous study [9], significant ASL CBF changes were not enhanced with general anesthesia in our study. The inhaled halogenated anesthetic, sevoflurane, is known to induce direct vasodilation of the cerebral vessels and could unbalance CBF reduction [29]. Furthermore, sevoflurane has a smaller vasodilation effect than other halogenated anesthetics and is less likely to induce brain luxury perfusion. These results suggest that sevoflurane should be preferred to other anesthetics in pediatric brain perfusion research.

Our workflow allowed fully automated processing of ASL data, adjusted to pediatric MRI conditions. A major feature of our processing workflow was the correction of subject motion, which is of particular importance in pediatric populations. A few abnormal or moved ASL repetitions could induce outlier values in the ASL CBF map. Sidaros et al [30] showed that regular motion correction was often insufficient in an infant population, and could cause strong corolla-shaped artifacts. Furthermore, regular motion correction requires the definition of excessive motion and the suppression or the correction of moved repetitions. The use of a robust estimator of the mean like Huber's M-estimator overcomes the drawbacks of regular motion correction to avoid outliers and artifacts induced by uncorrected corrupted ASL repetitions [18].

Our workflow included a few limitations such as the use of NIHPD templates, which had an age range (4.5-18.5 years) different to that of our population. CBF measurements in white matter were higher for 1 year and 2-3 years age groups. Consequently, a cross-contamination between gray matter and white matter CBF values was possible, although no visual segmentation errors were found between 6 months and 4 years.

The aim of this work was to provide CBF reference values that could be used in clinical practice or in research studies. However, the different approaches of ASL (pulsed, continuous, pseudocontinuous), the different available quantification models and the varying values of quantification parameters make this goal difficult to achieve. Consequently, we chose literature values for some parameters (blood T1, brain/blood partition coefficient) and a single compartment quantification model in the quantification step, which was simpler to handle in clinical practice. These choices could have induced quantification errors, the aforementioned parameters being higher during childhood than in adulthood. Given that the use of adult values leads to underestimation of CBF for the brain/blood partition coefficient and overestimation of CBF for blood T1, the effects are antagonistic in the quantification step permitting the employment of adult values as suggested by Wang et al. and Alsop et al [13,20].

All MRI examinations were acquired in a clinical setting. Therefore, subjects in our study were not strictly healthy children and it could have affected CBF values. However, exclusion criteria were defined so as to exclude all pathologies that may affect brain perfusion and morphological MRI examinations had to be normal. Moreover, it would have been ethically questionable to recruit healthy children for studies requiring general anesthesia or sedation.

In conclusion, we provided values of ASL CBF in the brain, gray matter, white matter, hemispheres, and lobes over a wide age range, showing approximatively inverted U-shaped changes in brain perfusion in gray matter over the course of childhood. No significant effect of gender or general anesthesia on pediatric ASL CBF was found, thus allowing the development of ASL to be considered in pediatric patients. Our CBF data shows inter-subject variability and are cross-sectional; a

longitudinal study would allow better modeling of the relationship between age and brain perfusion from birth to adulthood.

Appendix: Definition of lobes using AAL labels

Names of lobes	Names of labels in AAL	Number of RIGHT labels	Number of LEFT labels
Frontal	Precentral gyrus	2002	2001
	Superior frontal gyrus, dorsolateral	2102	2101
	Superior frontal gyrus, orbital part	2112	2111
	Middle frontal gyrus	2202	2201
	Middle frontal gyrus, orbital part	2212	2211
	Inferior frontal gyrus, opercular part	2302	2301
	Inferior frontal gyrus, triangular part	2312	2311
	Inferior frontal gyrus, orbital part	2322	2321
	Rolandic operculum	2332	2331
	Supplementary motor area	2402	2401
	Olfactory cortex	2502	2501
	Superior frontal gyrus, medial	2602	2601
	Superior frontal gyrus, medial orbital	2612	2611
	Gyrus rectus	2702	2701
	Paracentral Lobule	6402	6401
Temporal	Superior temporal gyrus	8112	8111
	Temporal pole: superior temporal gyrus	8122	8121
	Middle temporal gyrus	8202	8201
	Temporal pole: middle temporal gyrus	8212	8211
	Inferior temporal gyrus	8302	8301
	Heschl gyrus	8102	8101
Parietal	Superior parietal gyrus	6102	6101
	Inferior parietal gyrus	6202	6201
	Precuneus	6302	6301

	Angular gyrus	6222	6221
	Supramarginal gyrus	6212	6211
	Postcentral gyrus	6002	6001
Occipital	Superior occipital gyrus	5102	5101
	Middle occipital gyrus	5202	5201
	Inferior occipital gyrus	5302	5301
	Cuneus	5012	5011
	Calcarine fissure and surrounding cortex	5002	5001
	Lingual gyrus	5022	5021
	Fusiform gyrus	5402	5401
Limbic	Anterior cingulate and paracingulate gyri	4002	4001
	Median cingulate and paracingulate gyri	4012	4011
	Posterior cingulate gyrus	4022	4021
	Hippocampus	4102	4101
	Parahippocampal gyrus	4112	4111
Insular	Insula	3002	3001

REFERENCES:

[1] J.A. Detre, J.S. Leigh, D.S. Williams, A.P. Koretsky, Perfusion imaging, Magn. Reson. Med. 23 (1992) 37–45.

[2] L. Sokoloff, Localization of functional activity in the central nervous system by measurement of glucose utilization with radioactive deoxyglucose, J. Cereb. Blood Flow Metab. 1 (1981) 7–36.

[3] M. Proisy, B. Bruneau, C. Rozel, C. Tréguier, K. Chouklati, L. Riffaud, P. Darnault, J.-C. Ferré, Arterial spin labeling in clinical pediatric imaging, Diagn. Interv. Imaging. 97 (2016) 151–158.

[4] P. Wintermark, A. Hansen, M.C. Gregas, J. Soul, M. Labrecque, R.L. Robertson, S.K. Warfield, Brain perfusion in asphyxiated newborns treated with therapeutic hypothermia, AJNR Am. J. Neuroradiol. 32 (2011) 2023–2029.

[5] J. Chen, D.J. Licht, S.E. Smith, S.C. Agner, S. Mason, S. Wang, D.W. Silvestre, J.A. Detre, R.A. Zimmerman, R.N. Ichord, J. Wang, Arterial spin labeling perfusion MRI in pediatric arterial ischemic stroke: initial experiences, J. Magn. Reson. 29 (2009) 282–290.

[6] V. Dangouloff-Ros, C. Deroulers, F. Foissac, M. Badoual, E. Shotar, D. Grévent, R. Calmon, M. Pagès, J. Grill, C. Dufour, T. Blauwblomme, S. Puget, M. Zerah, C. Sainte-Rose, F. Brunelle, P. Varlet, N. Boddaert, Arterial Spin Labeling to Predict Brain Tumor Grading in Children: Correlations between Histopathologic Vascular Density and Perfusion MR Imaging, Radiology. 281 (2016) 553-566.

[7] J.B. De Vis, E.T. Petersen, L.S. de Vries, F. Groenendaal, K.J. Kersbergen, T. Alderliesten, J. Hendrikse, M.J.N.L. Benders, Regional changes in brain perfusion during brain maturation measured non-invasively with Arterial Spin Labeling MRI in neonates, Eur. J. Radiol. 82 (2013) 538–543.

[8] A.F. Duncan, A. Caprihan, E.Q. Montague, J. Lowe, R. Schrader, J.P. Phillips, Regional cerebral blood flow in children from 3 to 5 months of age, AJNR Am. J. Neuroradiol. 35 (2014) 593–598.

[9] L. Biagi, A. Abbruzzese, M.C. Bianchi, D.C. Alsop, A. Del Guerra, M. Tosetti, Age dependence of cerebral perfusion assessed by magnetic resonance continuous arterial spin labeling, J. Magn. Reson. 25 (2007) 696–702.

[10] Y. Taki, H. Hashizume, Y. Sassa, H. Takeuchi, K. Wu, M. Asano, K. Asano, H. Fukuda, R. Kawashima, Correlation between gray matter density-adjusted brain perfusion and age using brain MR images of 202 healthy children, Hum. Brain Mapp. 32 (2011) 1973–1985.

[11] P.W. Hales, J.M. Kawadler, S.E. Aylett, F.J. Kirkham, C.A. Clark, Arterial spin labeling characterization of cerebral perfusion during normal maturation from late childhood into adulthood: normal “reference range” values and their use in clinical studies, J. Cereb. Blood Flow Metab. 34 (2014) 776–784.

[12] B.B. Avants, J.T. Duda, E. Kilroy, K. Krasileva, K. Jann, B.T. Kandel, N.J. Tustison, L. Yan, M. Jog, R. Smith, Y. Wang, M. Dapretto, D.J.J. Wang, The pediatric template of brain perfusion, Sci. Data. 2 (2015) 150003.

[13] J. Wang, D.J. Licht, G.-H. Jahng, C.-S. Liu, J.T. Rubin, J. Haselgrove, R.A. Zimmerman, J.A. Detre, Pediatric perfusion imaging using pulsed arterial spin labeling, J. Magn. Reson. 18 (2003) 404–413.

[14] W.M. Luh, E.C. Wong, P.A. Bandettini, J.S. Hyde, QUIPSS II with thin-slice TI1 periodic saturation: a method for improving accuracy of quantitative perfusion imaging using pulsed arterial spin labeling, Magn. Reson. Med. 41 (1999) 1246–1254.

[15] S.M. Smith, Fast robust automated brain extraction, Hum. Brain Mapp. 17 (2002) 143–155.

[16] V. Fonov, A.C. Evans, K. Botteron, C.R. Almli, R.C. McKinstry, D.L. Collins, Brain Development Cooperative Group, Unbiased average age-appropriate atlases for pediatric studies, NeuroImage. 54 (2011) 313–327.

[17] K.J. Friston, C.D. Frith, R.S. Frackowiak, R. Turner, Characterizing dynamic brain responses with fMRI: a multivariate approach, NeuroImage. 2 (1995) 166–172.

[18] C. Maumet, P. Maurel, J.-C. Ferré, C. Barillot, Robust estimation of the cerebral blood flow in arterial spin labelling, Magn. Reson. Imaging. 32 (2014) 497–504.

[19] J. Wang, D.C. Alsop, L. Li, J. Listerud, J.B. Gonzalez-At, M.D. Schnall, J.A. Detre, Comparison of quantitative perfusion imaging using arterial spin labeling at 1.5 and 4.0 Tesla, Magn. Reson. Med. 48 (2002) 242–254.

[20] D.C. Alsop, J.A. Detre, X. Golay, M. Günther, J. Hendrikse, L. Hernandez-Garcia, H. Lu, B.J. MacIntosh, L.M. Parkes, M. Smits, M.J.P. van Osch, D.J.J. Wang, E.C. Wong, G. Zaharchuk, Recommended implementation of arterial spin-labeled perfusion MRI for clinical applications: A consensus of the ISMRM perfusion study group and the European consortium for ASL in dementia, Magn. Reson. Med. 73 (2015) 102–116.

[21] H.J.M.M. Mutsaerts, E. Richard, D.F.R. Heijtel, M.J.P. van Osch, C.B.L.M. Majoie, A.J. Nederveen, Gray matter contamination in arterial spin labeling white matter perfusion measurements in patients with dementia, NeuroImage Clin. 4 (2014) 139–144.

[22] N. Tzourio-Mazoyer, B. Landeau, D. Papathanassiou, F. Crivello, O. Etard, N. Delcroix, B. Mazoyer, M. Joliot, Automated anatomical labeling of activations in SPM using a macroscopic anatomical parcellation of the MNI MRI single-subject brain, NeuroImage. 15 (2002) 273–289.

[23] C. Chiron, C. Raynaud, B. Mazière, M. Zilbovicius, L. Laflamme, M.C. Masure, O. Dulac, M. Bourguignon, A. Syrota, Changes in regional cerebral blood flow during brain maturation in children and adolescents, J. Nucl. Med. 33 (1992) 696–703.

[24] M. Wintermark, D. Lepori, J. Cotting, E. Roulet, G. van Melle, R. Meuli, P. Maeder, L. Regli, F.R. Verdun, T. Deonna, P. Schnyder, F. Gudinchet, Brain perfusion in children: evolution with age assessed by quantitative perfusion computed tomography, Pediatrics. 113 (2004) 1642–1652.

[25] H.T. Chugani, M.E. Phelps, J.C. Mazziotta, Positron emission tomography study of human brain functional development, Ann. Neurol. 22 (1987) 487–497.

[26] T.D. Satterthwaite, R.T. Shinohara, D.H. Wolf, R.D. Hopson, M.A. Elliott, S.N. Vandekar, K. Ruparel, M.E. Calkins, D.R. Roalf, E.D. Gennatas, C. Jackson, G. Erus, K. Prabhakaran, C. Davatzikos, J.A. Detre, H. Hakonarson, R.C. Gur, R.E. Gur, Impact of puberty on the evolution of cerebral perfusion during adolescence, Proc. Natl. Acad. Sci. U. S. A. 111 (2014) 8643–8648.

[27] V. Jain, J. Duda, B. Avants, M. Giannetta, S.X. Xie, T. Roberts, J.A. Detre, H. Hurt, F.W. Wehrli, D.J.J. Wang, Longitudinal reproducibility and accuracy of pseudo-continuous arterial spin-labeled perfusion MR imaging in typically developing children, Radiology. 263 (2012) 527–536.

[28] L. Schlünzen, N. Juul, K.V. Hansen, G.E. Cold, Regional cerebral blood flow and glucose metabolism during propofol anaesthesia in healthy subjects studied with positron emission tomography, Acta Anaesthesiol. Scand. 56 (2012) 248–255.

[29] K.K. Kaisti, J.W. Långsjö, S. Aalto, V. Oikonen, H. Sipilä, M. Teräs, S. Hinkka, L. Metsähonkala, H. Scheinin, Effects of sevoflurane, propofol, and adjunct nitrous oxide on regional cerebral blood flow, oxygen consumption, and blood volume in humans, Anesthesiology. 99 (2003) 603–613.

[30] K. Sidaros, K. Olofsson, M.J. Miranda, O.B. Paulson, Arterial spin labeling in the presence of severe motion, J. Cereb. Blood Flow Metab. 25 (2005) S382.

TABLES:

Table 1

MRI indications for all children

MRI indications	*n*
Headache	24
Seizure	12
Brief minor neurological deficit without sequelae	10
Psychomotor retardation	9
Autism	8
Facial Port-Wine Stain	8
Paresthesia	4
Behavioral disorders	3
Others [a]	6
Total	84

Note: All MRI images must be normal and were performed outside an acute context; *n* number of patients.

[a] Others: cervical bone malformation, drug intoxication, psychological problem, uveitis, weight loss, chronic fatigue.

Table 2

CBF values for each age group in the brain, gray matter and white matter.

Age group	Brain CBF [a] Mean (±SE)	GM CBF [a] Mean (±SE)	WM CBF [a] Mean (±SE)	*n*	Sex ratio F/M	Sedation No/S/GA
6-11 months	53.3 (±7.8)	58.6 (±8.3)	29.2 (±5.1)	4	2/2	0/4/0
12-23 months	61.7 (±3.2)	68.2 (±3.5)	39.3 (±2.5)	14	5/9	0/14/0
2-3 years	68.5 (±4.4)	76.5 (±4.9)	40.2 (±4.5)	8	3/5	0/7/1
4-5 years	56.6 (±3.8)	64.9 (±4.3)	26.0 (±2.1)	13	4/9	1/2/10
6-7 years	62.4 (±3.0)	71.4 (±3.1)	30.5 (±2.3)	8	4/4	6/0/2
8-9 years	54.9 (±2.7)	63.9 (±3.1)	25.8 (±1.8)	11	6/5	10/0/1
10-11 years	53.4 (±5.2)	62.4 (±6.1)	23.9 (±2.6)	7	5/2	7/0/0
12-13 years	43.3 (±2.6)	51.0 (±3.0)	21.7 (±2.0)	11	7/4	9/0/2
14-15 years	50.1 (±2.0)	59.3 (±2.5)	24.8 (±1.2)	8	8/0	8/0/0
Total	56.1 (±1.4)	64.2 (±1.5)	29.3 (±1.1)	84	44/40	41/27/16

Note: CBF, cerebral blood flow; GM, gray matter; WM, white matter; *n* number of patients; SE, standard error of the means; F, female; M, male; S, sedative; GA, general anesthesia.

[a] CBF unit is mL/100 g/min.

Table 3

Results of the polynomial model comparison.

Model	Formula	-2 ln *L*	AIC	LRT	LRT p value	r	r p value
Linear	$CBF_{GM} = 71.50 – 1.01 \times age$	668	673.9	11.15	<0.001	0.35	0.001
Quadratic	$CBF_{GM} = 67.86 + 0.49 \times age - 0.09 \times age^2$	666	674.1	1.79	0.18	0.38	0.0003
Cubic	$CBF_{GM} = 60.74 + 5.82 \times age - 0.92 \times age^2 + 0.03 \times age^3$	663	**672.7**	3.42	0.06	0.42	<0.0001

Note: CBF, cerebral blood flow; GM, gray matter; -2 ln L, log-likelihood; AIC, Akaike information criterion; LRT, Likelihood Ratio test between model of order *k* and model of order *k-1* (e.g., for the linear model, the comparison is between linear model and model with intercept only); r, correlation coefficient.

Table 4

CBF values for each age group in lobes.

Age Group	Frontal lobe CBF[a] Mean (±SE) *n* = 82	Insular lobe CBF[a] Mean (±SE) *n* = 83	Limbic lobe CBF[a] Mean (±SE) *n* = 83	Occipital lobe CBF[a] Mean (±SE) *n* = 80	Parietal lobe CBF[a] Mean (±SE) *n* = 82	Temporal lobe CBF[a] Mean (±SE) *n* = 79
6-11 months	54.6 (±8.7)	55.8 (±7.7)	55.9 (±8.6)	69.9 (±6.2)	60.6 (±10.3)	62.8 (±8.8)
12-23 months	68.4 (±3.9)	66.0 (±4.0)	67.4 (±3.9)	75.2 (±3.3)	68.1 (±3.8)	75.3 (±4.1)
2-3 years	76.0 (±4.9)	71.2 (±4.4)	71.2 (±5.0)	86.2 (±5.3)	79.1 (±6.2)	81.7 (±5.0)
4-5 years	59.2 (±4.6)	60.5 (±4.9)	61.0 (±4.3)	78.4 (±5.9)	68.5 (±4.7)	68.4 (±4.6)
6-7 years	71.9 (±3.2)	65.0 (±4.1)	66.5 (±2.3)	78.0 (±4.1)	72.8 (±4.3)	80.7 (±4.4)
8-9 years	64.8 (±3.8)	56.9 (±3.2)	62.0 (±3.3)	70.2 (±2.7)	64.5 (±3.8)	69.9 (±3.9)
10-11 years	63.8 (±7.1)	54.4 (±6.5)	56.5 (±5.9)	72.2 (±4.9)	61.5 (±7.2)	65.4 (±6.5)
12-13 years	52.4 (±3.1)	48.7 (±3.2)	48.9 (±3.1)	54.8 (±3.6)	48.3 (±3.2)	56.1 (±4.0)
14-15 years	59.8 (±2.3)	55.8 (±2.5)	56.5 (±2.9)	66.2 (±3.8)	57.5 (±3.4)	64.8 (±3.3)
Total	63.5 (±1.6)	59.7 (±1.6)	61.1 (±1.5)	72.4 (±1.7)	64.6 (±1.8)	70.3 (±1.8)

Note: CBF, cerebral blood flow; *n*, number of patients; SE, standard error of the means.

[a] CBF unit is mL/100 g/min.

FIGURE CAPTIONS:

Figure 1. Changes in gray matter CBF as a function of age. Gray matter CBF was fitted using negative linear (blue line), quadratic (green line) and cubic polynomial regression (red line).

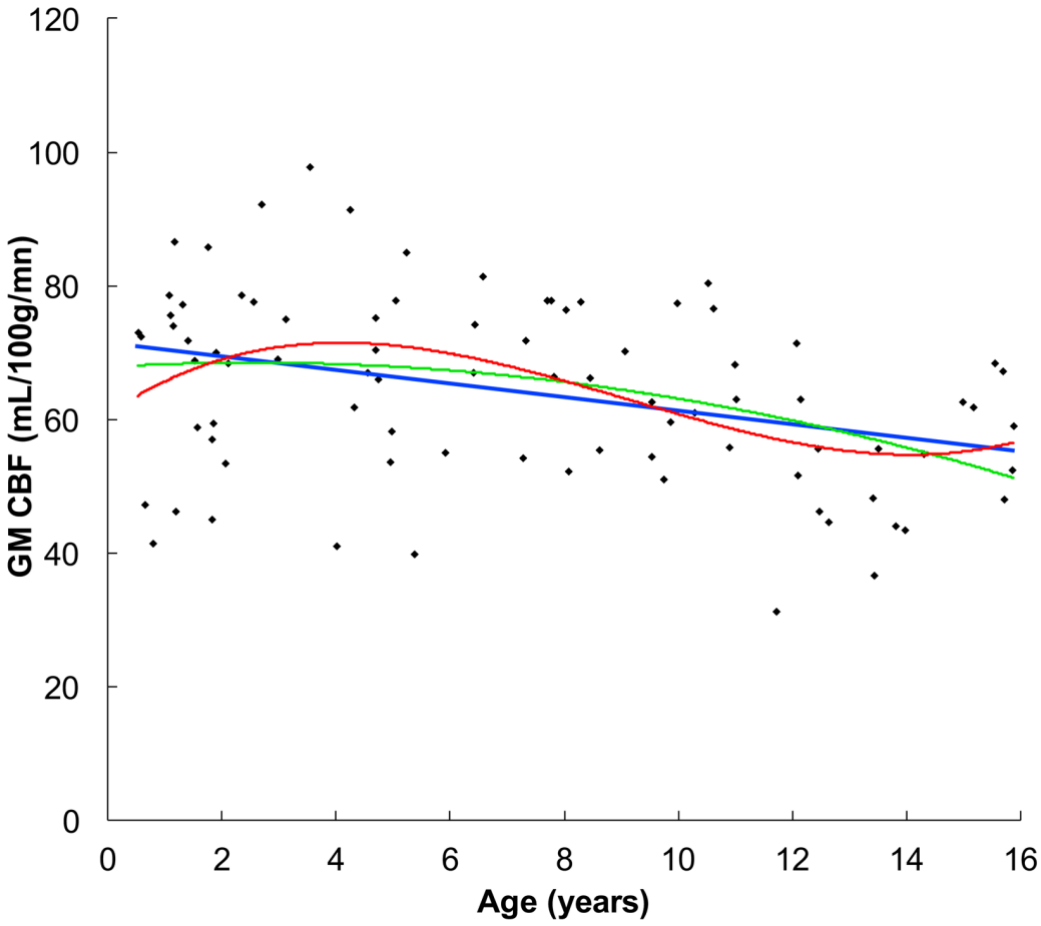

Figure 2. Examples of representative single subject ASL CBF map as a function of age. (A) child aged 6 months. (B) child aged 4 years. (C) child aged 7 years. (D) child aged 11 years. (E) child aged 15 years.

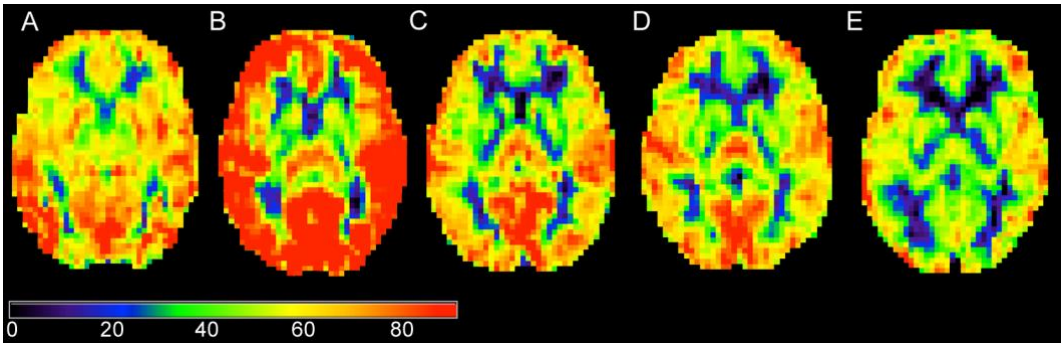

Figure 3. Lobes CBF values in all population. Only the significant differences between lobes founded by the Tukey's honestly significant difference test are shown. The number of stars designated the level of significance (*: $p < 0.05$; **: $p < 0.01$; ***: $p < 0.001$; ****: $p < 0.0001$).